

Engineering Div., Aluminum Co. of America, New Kensington, Pa.

² Westerlund, R. W. et al., "Development of a High Strength Aluminum Alloy, Readily Weldable in Plate Thicknesses and Suitable for Application at -423°F (-253°C)," Final Report on NASA Contract NAS-8-5452, Oct. 1967, Aluminum Co. of America, New Kensington, Pa.

A New Correlation of Parachute Weight Data

KENNETH E. FRENCH*

Lockheed Missiles & Space Company, Sunnyvale, Calif.

Nomenclature

D_0 = parachute reference (constructed) diam, ft or m

F_0 = parachute maximum opening force, lbf or N

k_i = coefficient of proportionality, dimensions as required ($i = 1-4$)

l_s = line length (from confluence point to canopy skirt), ft or m

N = number of suspension lines

P_c = rated ultimate strength of canopy material

P_s = rated ultimate strength of suspension line, lbf or N

q = dynamic pressure at chute deployment, lbf/ft² or N/m²

S_0 = parachute reference area, ft² or m²

W = weight, lbm or kg

Introduction

IN parachute and parachute system design, it is desirable to be able to rapidly assess nominal parachute weight, to estimate tolerances on the nominal weight, and to calculate weight tradeoffs with respect to variations in such parameters as parachute size and strength. This Note presents a correlation of parachute weight data to assist the designer in performing such tasks.

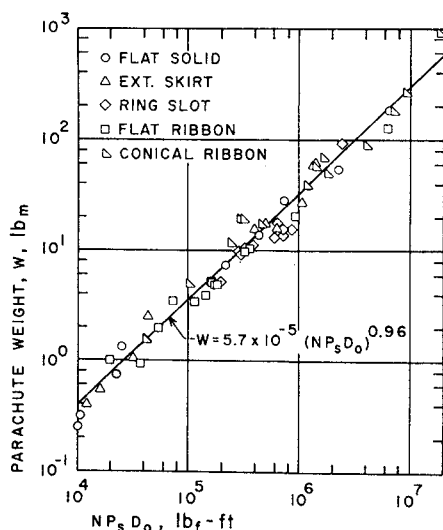


Fig. 1 Parachute weight vs $NP_s D_0$.

Received June 15, 1970; revision received August 5, 1970. This work was supported in part by the Lockheed Missiles & Space Company Independent Development Program.

* Staff Engineer, Advanced Design Department. Associate Fellow AIAA.

Rationale

Parachute weight can be considered to consist of two major parts: suspension line weight and canopy weight. Total suspension line weight will depend on the number, length, and material of the suspension lines. Canopy weight will depend on canopy area and material. Also, material weight is approximately proportional to material strength

Table 1 Parachute weight and configuration data

Type of chute	D_0 , ft	N	P_s , lbf	l_s/D_0	W , lbm	Use ^a
Flat solid	1.75	6	1,000		0.31	
	5	8	250		0.25	
	7.5	8	375		0.75	1
	10	10	250		1.31	
	24	24	375		7.5	
	28	28	550		14	2
	44	44	375		29	
	64	64	550		55.12	3
	100	100	550		186	
Ext. skirt	6	8	250		0.4	1
	8	8	250		0.54	1
	11.5	10	375		2.56	
	24	24	550		10.66	2
	32	36	550		16.25	4
	35	30	550		16	
	37.1	36	375		18	4
	44	44	550		27.5	
	67	52	375		58.75	
	67	56	375		63	
Ring slot	10.86 ^b	12	1,500	0.83	5.31	4
	14	20	2,250		15.5	
	15	20	1,000		9.5	5
	16	20	1,000		11	
	16	16	1,500		11.19	
	16	20	2,250		14	
	16	20	2,250		16	
	16	24	2,250		16	
	20	20	1,500		13.28	5
	29.6 ^b	24	400	0.90	9.88	4
Flat ribbon	29.6 ^b	24	900	1.00	18	4
	70	64	550		95	
	3	12	1,500		2	
	3.4	8	1,000		0.94	
	4.33	16	2,500		5	
	6	6	550		1	6
	6	16	1,500	1.33	4	
	6.05	8	1,500		3.5	4
	9	16	2,500		10.5	
Conical ribbon	11	28	3,000	1.00	21	
	11.5	10	1,000		3.5	1
	11.5	14	1,000		5.25	
	11.5	14	1,000		5.1	5
	15	16	750		5	
	16	20	1,000		10	
	43.5	48	3,000		129	
	4.82	14	1,500		5	4
	5.58	18	4,500		17.5	4
Conical ribbon	5.88	18	3,000		19.25	4
	6.86	8	750		1.56	4
	10.83	18	1,500		19.25	4
	12.5	16	9,000	1.12	50	
	13.3	18	1,000		11.75	4
	17	24	10,000	1.12	90	
	17.8	22	3,000		39	4
	20	30	12,000		180	
	29	32	1,500		57.3	4
	35	32	1,500		69	4
Conical ring slot parachute.	48	48	4,000	0.92	266	
	76	80	3,000		900	

^a Use code: 1 = flare descent, 2 = personnel, 3 = balloon payload recovery, 4 = aerospace vehicle recovery, 5 = aircraft landing brake, and 6 = antispin.

^b Conical ring slot parachute.

Table 2 Statistically derived variations

Range of values ($W_{\text{nominal}} = 1$)	Probability that actual weight is included in range (%)
0.83-1.21	50
0.75-1.33	68.3
0.58-1.74	95

for conventional materials. Thus, a general expression for parachute weight may be stated as

$$W_{\text{chute}} \approx k_1 NP_s l_s + k_2 P_s D_0^2 \quad (1)$$

Canopy strength will be compatible with total line strength for a well-designed chute. Thus, P_c may be taken as approximately proportional to NP_s . In addition, l_s is directly proportional to D_0 for conventionally configured parachutes. With these considerations, Eq. (1) may be restated in the form

$$W_{\text{chute}} \approx k_2 NP_s D_0 (1 + k_4 D_0) \quad (2)$$

Thus, $W_{\text{chute}} \propto NP_s D_0$ if $k_4 D_0 \ll 1$.

Correlation of Data

Table 1 lists weight and configuration data obtained from various sources¹⁻³ for 59 parachutes. Most of these chutes are of relatively conventional construction with $l_s/D_0 \approx 1$ and $N \approx D_0$ expressed in feet (at least for $D_0 > 10$ ft). Figure 1 shows weight vs $NP_s D_0$ on log-log scales for the parachutes of Table 1. The straight line shown in Fig. 1 is

$$W(\text{lbm}) = 0.57 \times 10^{-4} [NP_s D_0 (\text{lb-ft})]^{0.96} \quad (3a)$$

or

$$W(\text{kg}) = 1.9 \times 10^{-5} [NP_s D_0 (N - m)]^{0.96} \quad (3b)$$

The data scatter in Fig. 1 appears due as much to variations within each specific type of chute as to type-to-type variations. Thus, the incorporation of all types of chute in one graph appears valid.

Statistical methods⁴ applied to the data of Table 1 permit calculation of the variations and associated probabilities indicated in Table 2.

The spread associated with the calculated nominal value for chute weight tends to be large, but some of the spread is attributable to the inclusion of unconventional chute configurations in the data. Since 50% of the data are within +21%, -17% of the nominal, the nominal weight value of Eqs. (3) multiplied by 1.21 should provide a fairly conservative maximum weight for estimating purposes. Note, however, that the weights of Table 1, Fig. 1, and Eqs. (3) are for the parachute only; that is, riser, deployment bag, and special attachment link weights are excluded. Riser weight may be estimated as indicated in a previous work.⁵

Differentiation of the logarithm of Eqs. (3) gives the variation in W for small variations in N , P_s , and D_0 . For most chute applications, $F_0 \propto q S_0$ for small changes in deployment conditions and $NP_s \propto F_0$. Thus, $NP_s \propto q D_0^2$. Use of this relationship in Eqs. (3) and differentiation of the logarithm of the result can be used to obtain the variation in W for small variations in q and D_0 .

References

- 1 Pepper, W. B., Jr., "Parachute Design and Performance for Supersonic Deployment and for the Recovery of Heavy Loads," DGLR-DFVLR-AGARD Symposium, Sept. 15-19, 1969, Technical University of Braunschweig, Braunschweig, West Germany.
- 2 "X-7A Supersonic Ramjet Test Vehicle Parachute Recovery System," TR 55-162, June 1955, Wright Air Development Center, Wright-Patterson Air Force Base, Ohio.

³ Lindgren, M. J., private communication, May 1970.

⁴ Arkin, H. and Colton, R. R., *Statistical Methods*, 4th ed. revised, Barnes & Noble, New York, 1956, Chaps. IX and X.

⁵ French, K. E., "Drogue Parachute Weight," *Astronautics and Aerospace Engineering*, Vol. 1, No. 5, June 1963, pp. 94-95.

Equilibrium Vortex Positions

DONALD D. SEATH*

The University of Texas at Arlington, Arlington, Texas

VORTICES on the lee side of inclined cylindrical and conical bodies can cause significant departures of experimental data from inviscid slender-body theory. These vortices appear symmetrically in pairs, starting near the nose and growing in size and distance from the body as they trail downstream. Tinling and Allen¹ found one pair of counter-rotating vortices behind an ogive-cylinder body at subsonic speeds. Rainbird et al.² found up to three pairs of vortices behind an inclined circular cone in a water tunnel.

An examination of these body vortex flowfields in a plane perpendicular to the body axis (the crossflow plane) reveals a circular body with one, two, or three pairs of vortices on the lee side, and a crossflow velocity $U = V \sin \alpha$, where V is flight velocity and α is angle of attack. An idealized potential flow equation can be written for this flowfield, and, for the case of only one pair of vortices in the wake, an analytical solution has been obtained by Föppl³ for the equilibrium positions of these wake vortices. Details of this solution are given by Milne-Thomson.⁴

This Note presents equations and solutions for the equilibrium positions of multiple pairs of vortices in the wakes of circular and elliptic bodies.

Analysis

The complex potential for N pairs of vortices (and their images) of strength Γ_j , a doublet to represent a circular body of radius a , and a uniform stream of velocity U is (see Fig. 1)

$$w(z) = U \left(z + \frac{a^2}{z} \right) + \sum_{j=1}^N \left(\frac{i\Gamma_j}{2\pi} \right) \left[\ln(z - z_j) - \ln \left(z - \frac{a^2}{z_j^*} \right) - \ln(z - z_j^*) + \ln \left(z - \frac{a^2}{z_j} \right) \right] \quad (1)$$

where z^* is the complex conjugate of z . At an arbitrary point z_k , coinciding with one of the N vortices in the first quadrant,

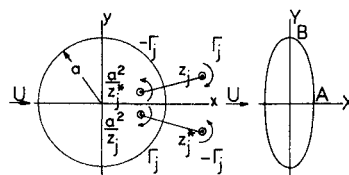


Fig. 1 Circle plane and ellipse plane.

Received August 17, 1970; revision received October 13, 1970. This work was supported in part by the National Science Foundation under Grant GK-940.

* Associate Professor of Aerospace Engineering. Associate Member AIAA.